

Lepton pair decays of the K_L meson in the light-front model

C. Q. Geng^{a,b} and C. W. Hwang^a

^a *Department of Physics, National Tsing Hua University, Hsinchu, Taiwan 300, ROC*

^b *Theory Group, TRIUMF, 4004 Wesbrook Mall, Vancouver, B.C. V6T 2A3, Canada*

Abstract

We analyze the K_L lepton pair decays of $K_L \rightarrow l^+l^-\gamma$ and $K_L \rightarrow l^+l^-l'^+l'^-$ ($l, l' = e, \mu$) within the framework of the light-front model. With the $K_L \rightarrow \gamma^*\gamma^*$ form factors evaluated in the model, we calculate the decay branching ratios of the modes and we find out that our results are all consistent with the experimental data. In addition, we have a discussion about the $K_L \rightarrow l^+l^-$ decay.

PACS numbers: 13.20.Eb, 12.39.Ki

The study of kaon decays has played a pivotal role in formulating the standard model of electroweak interactions [1]. In particular, the rare decay of $K_L \rightarrow \mu^+ \mu^-$ was used to constrain the flavor changing neutral current [2] as well as the top quark mass [3]. However, there are ambiguities in extracting the short-distance contribution since the long-distance contribution dominated by the two-photon intermediate state is not well known because its dispersive part cannot be calculated in a reliable way [4–7]. To have a better understanding of this dispersive part, it is important to study the lepton pair decays of the K_L meson such as $K_L \rightarrow l^+ l^- \gamma$ and $l^+ l^- l^+ l^-$ ($l = e, \mu$) since they can provide us with information on the structure of the $K_L \rightarrow \gamma^* \gamma^*$ vertex [4–7]. On the other hand, since these lepton pair decays are dominated by the long-distance physics, they can also be served as a testing ground for theoretical techniques such as chiral Lagrangian or other non-perturbative methods that seek to account for the low-energy behavior of QCD.

Recently, several new measurements of the decay branching ratios of $K_L \rightarrow \mu^+ \mu^- \gamma$, $K_L \rightarrow e^+ e^- e^+ e^-$, and $K_L \rightarrow e^+ e^- \mu^+ \mu^-$ have been reported [8–11]. These decays proceed entirely through the $K \gamma^* \gamma^*$ vertex and provide the best opportunity for the study of its form factor. In Ref. [12], since the assumption of neglecting the momentum dependence for the form factor was adopted, the results for the decays are only valid for those with only the electron-positron pair. In Ref. [13], the decays were studied at the order p^6 in Chiral Perturbation Theory (ChPT). However, all the results in Ref. [13] are smaller than the current experimental values. In this work, we use another non-perturbative method, the light-front quark model (LFQM) to analyze the $K \gamma^* \gamma^*$ form factor. As is well known [14], the LFQM is the relativistic quark model, which allows an exact separation in momentum space between the center-of-mass motion and intrinsic wave functions. A consistent treatment of quark spins and the center-of-mass motion can also be carried out. It has been successfully applied to calculate various form factors [15].

In this paper, we first derive the theoretical formalism for the decay constant and the $K \gamma^* \gamma^*$ vertex. We then use these formalism in the LFQM to extract the decay constant and the form factor.

We start with the K meson decay constant f_K , defined by

$$\langle 0 | A^\mu | K(P) \rangle = i f_K P^\mu, \quad (1)$$

where $A^\mu = \bar{u} \gamma^\mu \gamma_5 s$ is the axial vector current. Assuming a constant vertex function Λ_K [16,17] which is related to the $u\bar{s}$ bound state of the kaon. Then the quark-meson diagram, depicted in Fig. 1 (a), yields

$$\langle 0 | A^\mu | K(P) \rangle = -\sqrt{N_c} \int \frac{d^4 p_1}{(2\pi)^4} \Lambda_K \text{Tr} \left[\gamma_5 \frac{i(\not{p}_2 + m_s)}{p_2^2 - m_s^2 + i\epsilon} \gamma^\mu \gamma_5 \frac{i(\not{p}_1 + m_u)}{p_1^2 - m_u^2 + i\epsilon} \right], \quad (2)$$

where $m_{u,s}$ are the masses of u and s quark, respectively, and N_c is the number of colors. We consider the poles in denominators in terms of the LF coordinates (p^-, p^+, p_\perp) and perform the integration over the LF “energy” p_1^- in Eq. (6). The result is

$$\langle 0 | A^\mu | K(P) \rangle = \sqrt{N_c} \int \frac{[d^3 p_1]}{p_1^+ p_2^+} \frac{\Lambda_{KL}}{P^- - p_{1\text{on}}^- - p_{2\text{on}}^-} (I_1^\mu |_{p_1^- = p_{1\text{on}}^-}), \quad (3)$$

where

$$[d^3 p_1] = \frac{dp_1^+ d^2 p_{1\perp}}{2(2\pi)^3}, \quad p_{\text{ion}}^- = \frac{m_i^2 + p_{i\perp}^2}{p_i^+},$$

$$I_1^\mu = \text{Tr}[\gamma_5(\not{p}_2 + m_s)\gamma^\mu\gamma_5(\not{p}_1 + m_u)]. \quad (4)$$

For $K_L \rightarrow \gamma^* \gamma^*$, by assuming CP conservation the amplitude is given by

$$A(K_L \rightarrow \gamma^*(q_1, \epsilon_1) \gamma^*(q_2, \epsilon_2)) = iF(q_1^2, q_2^2) \varepsilon_{\mu\nu\rho\sigma} \epsilon_1^\mu \epsilon_2^\nu q_1^\rho q_2^\sigma, \quad (5)$$

where the form factor of $F(q_1^2, q_2^2)$ in Eq. (5) is a symmetric function under the interchange of q_1^2 and q_2^2 . Using the same procedure as above, the quark-meson diagram depicted in Fig. 2 yields

$$A(K_L \rightarrow \gamma^* \gamma^*) = - \int \frac{d^4 p_1}{(2\pi)^4} \Lambda_{K_L} \left\{ \text{Tr} \left[\gamma_5 \frac{i(\not{p}_3 + m_s)}{p_3^2 - m_s^2 + i\epsilon} \not{\epsilon}_2 \frac{i(\not{p}_2 + m_s)}{p_2^2 - m_s^2 + i\epsilon} \right. \right. \\ \left. \left. \times C_W(q_1^2) \not{\epsilon}_1 \frac{i(\not{p}_1 + m_d)}{p_1^2 - m_d^2 + i\epsilon} + (d \leftrightarrow s) \right] + (\epsilon_1 \leftrightarrow \epsilon_2) \right\}, \quad (6)$$

where $p_2 = p_1 - q_1$ and $p_3 = p_1 - P$, and C_W is the effective contribution to the inclusive $s \rightarrow d\gamma^*$ decay. After integrating over p_1^- , we obtain

$$A(K_L \rightarrow \gamma^* \gamma^*) = \left\{ \left[\int_0^{q_1} \frac{[d^3 p_1]}{\prod_{i=1}^3 p_i^+} \frac{\Lambda_{K_L}}{P^- - p_{1\text{on}}^- - p_{3\text{on}}^-} (I|_{p_1^- = p_{1\text{on}}^-}) \frac{C_W(q_1^2)}{q_1^- - p_{1\text{on}}^- - p_{2\text{on}}^-} \right. \right. \\ \left. \left. + \int_{q_1}^P \frac{[d^3 p_1]}{\prod_{i=1}^3 p_i^+} \frac{\Lambda_{K_L}}{P^- - p_{1\text{on}}^- - p_{3\text{on}}^-} (I|_{p_3^- = p_{3\text{on}}^-}) \frac{C_W(q_1^2)}{q_2^- - p_{2\text{on}}^- - p_{3\text{on}}^-} + (d \leftrightarrow s) \right] \right. \\ \left. + (\epsilon_1 \leftrightarrow \epsilon_2) \right\}, \quad (7)$$

where $q_2^- = P^- - q_1^-$ and

$$I_2 = \text{Tr}[\gamma_5(\not{p}_3 + m_s) \not{\epsilon}_2(\not{p}_2 + m_s) \not{\epsilon}_1(\not{p}_1 + m_d)]. \quad (8)$$

As describing in Ref. [18], the vertex function Λ_{K_L} and the denominators in Eq. (7) correspond to the K_L meson bound state. In the LFQM, the internal structure of the meson bound state [19–21] consists of ϕ , which describes the momentum distribution of the constituents in the bound state, and $R_{\lambda_1, \lambda_2}^{S, S_z}$, which creates a state of definite spin (S, S_z) out of LF helicity (λ_1, λ_2) eigenstates and is related to the Melosh transformation [22]. A convenient approach relating these two parts is shown in Ref. [18]. The interaction Hamiltonian is assumed to be $H_I = i \int d^3 x \bar{\Psi} \gamma_5 \Psi \Phi$ where Ψ is the quark field and Φ is the meson field containing ϕ and $R_{\lambda_1, \lambda_2}^{S, S_z}$. When considering the normalization of the meson state depicted in Fig. 1 (b) in the LFQM, we obtain

$$\langle M(P', S', S'_z) | H_I H_I | M(P, S, S_z) \rangle = 2(2\pi)^3 \delta^3(P' - P) \delta_{S S'} \delta_{S_z S'_z} \\ \times \int [d^3 p_1] \phi^2 R_{\lambda_1, \lambda_2}^{S, S_z} R_{\lambda_1, \lambda_2}^{S', S'_z} \text{Tr} \left[\gamma_5 \frac{-\not{p}_2 + m_2}{p_2^+} \gamma_5 \frac{\not{p}_1 + m_1}{p_1^+} \right]. \quad (9)$$

If we normalize the meson state and the momentum distribution function ϕ as [19]

$$\langle M(P', S', S'_z) | H_I H_I | M(P, S, S_z) \rangle = 2(2\pi)^3 P^+ \delta^3(P' - P) \delta_{SS'} \delta_{S_z S'_z}, \quad (10)$$

and

$$\int \frac{d^3 p_1}{2(2\pi)^3} \frac{1}{P^+} |\phi|^2 = 1, \quad (11)$$

respectively, where p_1 and p_2 are the on-mass-shell momenta, we have that

$$R_{\lambda_1, \lambda_2}^{S, S_z} = \frac{\sqrt{p_1^+ p_2^+}}{2\sqrt{p_{1\text{on}} \cdot p_{2\text{on}} + m_1 m_2}}. \quad (12)$$

The wave function and the Melosh transformation of the meson are related to the bound state vertex function Λ_M by

$$\frac{\Lambda_M}{P^- - p_{1\text{on}}^- - p_{2\text{on}}^-} \longrightarrow R_{\lambda_1, \lambda_2}^{S, S_z} \phi_M. \quad (13)$$

We note that p_1 , p_2 and p_3 in the trace of $I_{1,2}$ must be on the mass shell for self-consistency. After taking the ‘‘good’’ component $\mu = +$, we use the definitions of the LF momentum variables $(x, x', k_\perp, k'_\perp)$ [20] and take a Lorentz frame where $P_\perp = P'_\perp = 0$ to have $q_\perp = 0$ and $k'_\perp = k_\perp$. The decay constant f_K and the form factor $F(q_1^2, q_2^2)$ can be extracted by comparing these results with Eqs. (1) and (5), respectively, *i.e.*,

$$f_K = 2\sqrt{2}\sqrt{N_c} \int \frac{dx d^2 k_\perp}{2(2\pi)^3} \frac{\phi_{K_L}(x, k_\perp)}{\sqrt{a^2 + k_\perp^2}} a, \quad (14)$$

and

$$F(q_1^2, q_2^2) = \int \frac{d^2 k_\perp}{2(2\pi)^3} \left\{ C_W(q_1^2) \left[\int_0^{r_+} dx \frac{\phi_{K_L}(x, k_\perp)}{\sqrt{a^2 + k_\perp^2}} \frac{a[r_+/(r_+ - x)]}{\frac{m_s^2 + k_\perp^2}{(x/r_+)} + \frac{m_s^2 + k_\perp^2}{1 - (x/r_+)} - q_2^2} \right. \right. \\ \left. \left. + \int_{r_+}^1 dx \frac{\phi_{K_L}(x, k_\perp)}{\sqrt{a^2 + k_\perp^2}} \frac{a[(1 - r_+)/(x - r_+)]}{\frac{m_d^2 + k_\perp^2}{(1-x)/(1-r_+)} + \frac{m_s^2 + k_\perp^2}{(x-r_+)/(1-r_+)} - q_1^2} \right] + (d \leftrightarrow s) \right\} \\ + (q_1 \leftrightarrow q_2; r_+ \leftrightarrow 1 - r_-), \quad (15)$$

where

$$a = m_{u,d}x + m_s(1 - x), \quad m_u = m_d, \\ r_\pm = \frac{1}{2M_{K_L}^2} [M_{K_L}^2 + q_1^2 - q_2^2 \pm \sqrt{(M_{K_L}^2 + q_1^2 - q_2^2)^2 - 4M_{K_L}^2 q_1^2}], \quad (16)$$

and x is the momentum fraction carried by the spectator antiquark in the initial state.

In principle, the momentum distribution amplitude $\phi(x, k_\perp)$ can be obtained by solving the LF QCD bound state equation [23]. However, before such first-principle solutions are available, we shall have to use phenomenological amplitudes. One momentum distribution function that has often been used in the literature for mesons is the Gaussian-type,

$$\phi(x, k_{\perp})_{\text{G}} = \mathcal{N} \sqrt{\frac{dk_z}{dx}} \exp\left(-\frac{\vec{k}^2}{2\omega^2}\right), \quad (17)$$

where $\mathcal{N} = 4(\pi/\omega^2)^{3/4}$ and k_z is of the internal momentum $\vec{k} = (\vec{k}_{\perp}, k_z)$, defined through

$$1 - x = \frac{e_1 - k_z}{e_1 + e_2}, \quad x = \frac{e_2 + k_z}{e_1 + e_2}, \quad (18)$$

with $e_i = \sqrt{m_i^2 + \vec{k}^2}$. We then have

$$M_0 = e_1 + e_2, \quad k_z = \frac{xM_0}{2} - \frac{m_2^2 + k_{\perp}^2}{2xM_0}, \quad (19)$$

and

$$\frac{dk_z}{dx} = \frac{e_1 e_2}{x(1-x)M_0}, \quad (20)$$

which is the Jacobian of the transformation from (x, k_{\perp}) to \vec{k} .

To examine numerically the form factor derived in Eq. (15), we need to specify the parameters appearing in $\phi_M(x, k_{\perp})$. We shall use the decay constant $f_K = 159.8 \pm 1.5$ MeV [24] with the quark masses of m_d and m_s to constrain the scale parameter ω in Eq. (17). By using $m_s = 500 \pm 50$ MeV and $m_s - m_d = 180$ MeV [25], we find that ω is fixed to be $0.335_{-0.015}^{+0.027}$ GeV. Now, we use the momentum distribution functions $\phi(x, k_{\perp})_{\text{G}}$ to calculate the form factors $F(q_1^2, q_2^2)$ in time-like region of $0 \leq q_1^2$ and $q_2^2 \leq M_K^2 \simeq 0.25$ GeV². In this low energy region, we neglect the momentum dependence of the effective vertex $C_W(q^2)$ in Eq. (15), that is,

$$C_W(q^2) \simeq C_W(0). \quad (21)$$

We can use Eqs. (15) and (21) to get the function $f(y) \equiv F(q_1^2, 0)/F(0, 0)$, where $y \equiv q_1^2/M_K^2$, and the result is shown in Fig. 3. From the figure, we see that our result with the assumption of Eq. (21) agrees well with experimental data [26–28], in particular, in the lower y region. To get a better fit for a larger y , we may use

$$C_W(q^2) \simeq \frac{C_W(0)}{1 - \frac{q^2}{m_c^2}}, \quad (22)$$

and the result is also given in Fig. 3. We shall refer the two equations in (21) and (22) as Models (I) and (II), respectively.

This function of $f(y)$ is related to the differential decay rate of $K_L^0 \rightarrow l^+ l^- \gamma$ by

$$\frac{d\mathcal{B}_{l^+ l^- \gamma}}{dq_1^2} \equiv \frac{d\Gamma(K_L \rightarrow l^+ l^- \gamma)}{\Gamma(K_L \rightarrow \gamma \gamma) dq_1^2} = \frac{2}{q_1^2} \left(\frac{\alpha}{3\pi}\right) |f(y)|^2 \lambda^{3/2} \left(1, \frac{q_1^2}{M_{K_L}^2}, 0\right) G_l(q_1^2), \quad (23)$$

where

$$\lambda(a, b, c) = a^2 + b^2 + c^2 - 2(ab + bc + ca), \quad (24)$$

and

$$G_l(q^2) = \left(1 - \frac{4M_l^2}{q^2}\right)^{1/2} \left(1 + \frac{2M_l^2}{q^2}\right). \quad (25)$$

Integrating over q_1^2 in Eq. (23), we get the branching ratios

$$\begin{aligned} \mathcal{B}_{e^+e^-\gamma} &\equiv \frac{\Gamma(K_L^0 \rightarrow e^+e^-\gamma)}{\Gamma(K_L^0 \rightarrow \gamma\gamma)} = 1.64, \quad 1.65 \times 10^{-2}, \\ \mathcal{B}_{\mu^+\mu^-\gamma} &\equiv \frac{\Gamma(K_L^0 \rightarrow \mu^+\mu^-\gamma)}{\Gamma(K_L^0 \rightarrow \gamma\gamma)} = (5.66_{-0.09}^{+0.07}), \quad (5.90_{-0.10}^{+0.08}) \times 10^{-4}, \end{aligned} \quad (26)$$

for (I) and (II), respectively. These values agree well with the experimental data: $\mathcal{B}_{e^+e^-\gamma}^{\text{exp}} = (1.69 \pm 0.13) \times 10^{-2}$ [24] and $\mathcal{B}_{\mu^+\mu^-\gamma}^{\text{exp}} = (6.11 \pm 0.31) \times 10^{-4}$ [8], where we have used [29]

$$\Gamma^{\text{exp}}(K_L^0 \rightarrow \gamma\gamma) = [(5.92 \pm 0.15) \times 10^{-4}] \Gamma^{\text{exp}}(K_L^0 \rightarrow \text{all}). \quad (27)$$

On the other hand, our results are larger than $\mathcal{B}_{e^+e^-\gamma} = 1.59 \times 10^{-2}$ and $\mathcal{B}_{\mu^+\mu^-\gamma} = 4.09 \times 10^{-4}$ obtained in Ref. [12], where the momentum dependence of the form factor was neglected, i.e., $f(y) = 1$. This inconsistency is reasonable because the kinematic factor $G_l(q^2)$ which leads the contribution at $q^2 \simeq 4M_l^2$ is important, and the electron mass is very small so that $f(y) = 1$ is only valid for the decay with an electron-positron pair. For the muonic pair case, the mass of muon is not small, therefore the effect of the deviation of neglecting the momentum dependence is evident. This situation also occurs in the decays with two lepton pairs.

Next, Eq. (15) can be also used to calculate the differential decay rates of $K_L \rightarrow l^+l^-l'^+l'^-$ by

$$\frac{d\Gamma(K_L \rightarrow l^+l^-l'^+l'^-)}{\Gamma(K_L \rightarrow \gamma\gamma) dq_1^2 dq_2^2} = \frac{2}{q_1^2 q_2^2} \left(\frac{\alpha}{3\pi}\right)^2 \left| \frac{F(q_1^2, q_2^2)}{F(0, 0)} \right|^2 \lambda^{3/2} \left(1, \frac{q_1^2}{M_{K_L}^2}, \frac{q_2^2}{M_{K_L}^2}\right) G_l(q_1^2) G_{l'}(q_2^2). \quad (28)$$

After the integrations over q_1^2 and q_2^2 , for (I) and (II) we obtain the branching ratios as follows:

$$\begin{aligned} \mathcal{B}_{e^+e^-e^+e^-} &\equiv \frac{\Gamma(K_L^0 \rightarrow e^+e^-e^+e^-)}{\Gamma(K_L^0 \rightarrow \gamma\gamma)} = (6.63 \pm 0.01), \quad (6.68 \pm 0.01) \times 10^{-5}, \\ \mathcal{B}_{\mu^+\mu^-e^+e^-} &\equiv \frac{\Gamma(K_L^0 \rightarrow \mu^+\mu^-e^+e^-)}{\Gamma(K_L^0 \rightarrow \gamma\gamma)} = (4.00_{-0.08}^{+0.06}), \quad (4.17_{-0.08}^{+0.06}) \times 10^{-6}, \\ \mathcal{B}_{\mu^+\mu^-\mu^+\mu^-} &\equiv \frac{\Gamma(K_L^0 \rightarrow \mu^+\mu^-\mu^+\mu^-)}{\Gamma(K_L^0 \rightarrow \gamma\gamma)} = (1.68_{-0.11}^{+0.08}), \quad (1.77_{-0.12}^{+0.08}) \times 10^{-9}. \end{aligned} \quad (29)$$

In Table 1, we summary the experimental and theoretical values of the decay branching ratios for the K_L lepton pair modes. The results of Ref. [12] correspond a point-like form factor, while those in Ref. [13] are calculated at $O(p^6)$ in the ChPT.

Table 1: Summary of the lepton pair decays of K_L .

Br	PDG [24]	new data	Model (I)	Model (II)	Ref. [12]	Ref. [13]
$10^2 \times \mathcal{B}_{e^+e^-\gamma}$	1.69 ± 0.09		1.64	1.65	1.59	1.60 ± 0.15
$10^4 \times \mathcal{B}_{\mu^+\mu^-\gamma}$	5.49 ± 0.49	6.11 ± 0.31 [8]	$5.66^{+0.07}_{-0.09}$	$5.90^{+0.08}_{-0.10}$	4.09	4.01 ± 0.57
$10^5 \times \mathcal{B}_{e^+e^+e^-e^-}$	6.93 ± 0.20	6.28 ± 0.65 [9] 6.20 ± 0.69 [10]	6.63 ± 0.01	6.68 ± 0.01	5.89	6.50
$10^6 \times \mathcal{B}_{\mu^+\mu^-e^+e^-}$	$4.9^{+11.3}_{-4.0}$	4.43 ± 0.84 [11]	$4.00^{+0.06}_{-0.08}$	$4.17^{+0.06}_{-0.08}$	1.42	2.20 ± 0.25
$10^9 \times \mathcal{B}_{\mu^+\mu^-\mu^+\mu^-}$			$1.68^{+0.08}_{-0.11}$	$1.77^{+0.08}_{-0.12}$	0.946	1.30 ± 0.15

From Table 1, we may also combine the experimental values by assuming that they are uncorrelated and we find that

$$\begin{aligned}
 \mathcal{B}_{K_L \rightarrow \mu^+\mu^-\gamma}^{\text{exp}} &= (5.93 \pm 0.26) \times 10^{-4}, \\
 \mathcal{B}_{K_L \rightarrow e^+e^-e^+e^-}^{\text{exp}} &= (6.83 \pm 0.19) \times 10^{-5}, \\
 \mathcal{B}_{K_L \rightarrow \mu^+\mu^-e^+e^-}^{\text{exp}} &= (4.44^{+0.84}_{-0.82}) \times 10^{-6}.
 \end{aligned} \tag{30}$$

It is interesting to see that our results for $K_L \rightarrow l^+l^-\gamma$ are larger than those in Refs. [12,13] and they agree very well with the experimental data. Furthermore, as shown in Eq. (29), those for $K_L \rightarrow e^+e^-e^+e^-$ and $K_L \rightarrow \mu^+\mu^-e^+e^-$ also agree with the combined experimental values in Eq. (30). Here we do not consider the interference effect [12,13] from the identical leptons in the final state. The reasons are the followings. When we use the non-point-like form factor, this effect is about 0.5% in the $e^+e^-e^+e^-$ mode [13], which is beyond experimental access, while for the $\mu^+\mu^-e^+e^-$ mode, the relative size of the interference effect is larger, but it is outside the scope of future experiments because the total branching ratio for this decay is predicted to be about 8×10^{-13} .

We now use the form factor $F(q_1^2, q_2^2)$ to calculate the decays of $K_L \rightarrow l^+l^-$. The decay branching ratios of the modes can be generally decomposed in the following way

$$\mathcal{B}_{l^+l^-} \equiv \frac{\Gamma(K_L \rightarrow l^+l^-)}{\Gamma(K_L \rightarrow \gamma\gamma)} = |\text{Im } \mathcal{A}_l|^2 + |\text{Re } \mathcal{A}_l|^2, \tag{31}$$

where $\text{Im } \mathcal{A}_l$ denotes the absorptive contribution and $\text{Re } \mathcal{A}_l$ the dispersive one. The former can be determined in a model-independent form of

$$|\text{Im } \mathcal{A}_l|^2 = \frac{\alpha^2 M_l^2}{2 M_{K_L}^2 \beta_l} \left[\ln \frac{1 - \beta_l}{1 + \beta_l} \right]^2, \tag{32}$$

where $\beta_l^2 \equiv 1 - 4M_l^2/M_{K_L}^2$. The latter, however, can be rewritten as the sum of short-distance (SD) and long-distance (LD) contributions,

$$\text{Re } \mathcal{A}_l = \text{Re } \mathcal{A}_{l\text{SD}} + \text{Re } \mathcal{A}_{l\text{LD}}. \tag{33}$$

In the standard model, the SD part has been identified as the weak contribution represented by one-loop W -box and Z -exchange diagrams [3,30,31], while the LD one is related to $F(q_1^2, q_2^2)$ by

$$|\text{Re } \mathcal{A}_{l\text{LD}}|^2 = \frac{2\alpha^2 M_l^2 \beta_l}{\pi^2 M_{K_L}^2} |\text{Re } \mathcal{R}_l(M_{K_L}^2)|^2, \quad (34)$$

where [32]

$$\mathcal{R}_l(P^2) = \frac{2i}{\pi^2 M_K^2} \int d^4 q \frac{[P^2 q^2 - (P \cdot q)^2]}{q^2 (P - q)^2 [(q - p_l)^2 - M_l^2]} \frac{F(q^2, (P - q)^2)}{F(0, 0)}. \quad (35)$$

In general, an once-subtracted dispersion relation can be written for $\text{Re } \mathcal{R}$ as [33]

$$\text{Re } \mathcal{R}_l(P^2) = \text{Re } \mathcal{R}_l(0) + \frac{P^2}{\pi} \int_0^\infty dP'^2 \frac{\text{Im } \mathcal{R}_l(P'^2)}{(P'^2 - P^2)P'^2}, \quad (36)$$

where $\text{Re } \mathcal{R}_l(0)$ can be obtained by applying Eq. (15) in the soft limit, $P \rightarrow 0$.

For the $K_L \rightarrow e^+ e^-$ decay, using Eqs. (21) and (22) of Models (I) and (II) we find that

$$|\text{Re } \mathcal{A}_{e\text{LD}}|^2 = (5.41 \pm 0.12), \quad (5.81_{-0.08}^{+0.10}) \times 10^{-9}, \quad (37)$$

respectively. Since the SD part of $\text{Re } \mathcal{A}_{e\text{SD}}$ can be neglected, we get

$$\begin{aligned} \mathcal{B}_{e^+e^-}^I &= (1.07 \pm 0.01) \times 10^{-8}, \\ \mathcal{B}_{e^+e^-}^{II} &= (1.11 \pm 0.01) \times 10^{-8}, \end{aligned} \quad (38)$$

where we have used $|\text{Im } \mathcal{A}_e|^2 = 5.32 \times 10^{-9}$. Both results in Eq. (38) are consistent with the experimental value of $\mathcal{B}_{e^+e^-}^{\text{exp}} = (1.5_{-0.7}^{+1.0}) \times 10^{-8}$ measured by E871 at BNL [34], but it is lower than the value of $(1.52 \pm 0.09) \times 10^{-8}$ given by the calculation in Ref. [5] with the ChPT.

For the $K_L \rightarrow \mu^+ \mu^-$ decay, by subtracting between the value of $|\text{Im } \mathcal{A}_\mu|^2 = 1.20 \times 10^{-5}$ from the experimental data of $\mathcal{B}_{\mu^+\mu^-}^{\text{exp}} = (1.21 \pm 0.04) \times 10^{-5}$ [24,35], we obtain that

$$|\text{Re } \mathcal{A}_\mu|^2 \leq 7.2 \times 10^{-7} \quad (90\% \text{ C.L.}). \quad (39)$$

In the standard model, we have that [7,36]

$$|\text{Re } \mathcal{A}_{\mu\text{SD}}|^2 \mathcal{B}_{K_L \rightarrow \gamma\gamma} = 0.9 \times 10^{-10} (1.2 - \bar{\rho})^2 \left[\frac{\bar{m}_t(m_t)}{170 \text{ GeV}} \right]^{3.1} \left[\frac{|V_{cb}|}{0.040} \right]^4, \quad (40)$$

where $\bar{\rho} = \rho(1 - \lambda^2/2)$. Using the parameters of $\bar{m}_t(m_t) = 166 \pm 5 \text{ GeV}$, $|V_{cb}| = 0.041 \pm 0.002$ and $\bar{\rho} = 0.224 \pm 0.038$ [31,37], from Eqs. (27) and (40) we get

$$\text{Re } \mathcal{A}_{\mu\text{SD}} = -(1.22 \pm 0.17) \times 10^{-3}, \quad (41)$$

which is larger than the limit in Eq. (39). It is clear that the value of $\text{Re } \mathcal{A}_{\mu\text{LD}}$ has to be either very small for the same sign as $\text{Re } \mathcal{A}_{\mu\text{SD}}$ or the same order but for the opposite sign. For Model (I), from Eq. (36) we find

$$\text{Re } \mathcal{A}_{\mu\text{LD}}^I = -(1.34_{-0.16}^{+0.15}) \times 10^{-3}, \quad (42)$$

which is very close to the SD value in Eq. (41) and clearly ruled out if the absolute sign in Eqs. (41) and (42) are the same. However, if the relative sign is opposite, the limit in Eq. (39) is satisfied and it seems that no useful constraint can be extracted.

Similarly, for Model (II) we obtain

$$\text{Re } \mathcal{A}_{\mu\text{LD}}^{II} = -(8.26_{-1.08}^{+1.01}) \times 10^{-4}, \quad (43)$$

which leads to

$$|\text{Re } \mathcal{A}_{\mu\text{LD}}^{II}| \sqrt{\mathcal{B}_{K_L \rightarrow \gamma\gamma}} \leq 2.4 \times 10^{-5} \quad (90\% \text{ C.L.}). \quad (44)$$

We note that the limit in Eq. (44) is similar to that in Eq. (39) of Ref. [7]. This result is not surprising. If we fit $F(q_1^2, q_2^2)$ in Eq. (15) with Eq. (14) of Ref. [7] given by

$$f(q_1^2, q_2^2) = \frac{F(q_1^2, q_2^2)}{F(0, 0)} = 1 + \alpha \left(\frac{q_1^2}{q_1^2 - m_\rho^2} + \frac{q_2^2}{q_2^2 - m_\rho^2} \right) + \beta \frac{q_1^2 q_2^2}{(q_1^2 - m_\rho^2)(q_2^2 - m_\rho^2)}, \quad (45)$$

we find that $\alpha = -0.654$ and $\beta = 0.263$ and

$$1 + 2\alpha + \beta = -0.045, \quad (46)$$

which satisfies the bound of Eq. (35) in Ref. [7].

However, at the moment, we still not be able to get a useful constraint on the SD part. It is clear that more studies for the form of $C_W(q^2)$ are needed [38] before we can extract the short distance component of $K_L \rightarrow \mu^+ \mu^-$. Nevertheless, our approach here provides another useful tool for the K_L lepton pair decays beside of the ChPT.

In conclusion, we have studied the K_L lepton pair decays of $K_L \rightarrow l^+ l^- \gamma$ and $K_L \rightarrow l^+ l^- l'^+ l'^-$ in the light-front framework. In our calculations, we have adopted the Gaussian-type wave function and some assumptions about the momentum dependences of the effective vertex $C_W(q^2)$ in the low energy region. After fixing the parameters appearing in the wave function, we have found that the decay branching ratios of $K_L \rightarrow e^+ e^-$, $l^+ l^- \gamma$ and $e^+ e^- l^+ l^-$ ($l = e, \mu$) are all consistent with the experimental data. The remarkable agreement indicated that our assumptions in Eqs. (21) and (22) are quite reasonable. However, we still cannot get a useful constraint on the CKM parameters from the $K_L \rightarrow \mu^+ \mu^-$ decay.

ACKNOWLEDGMENTS

We would like to thank K. Terasaki for useful data. This work was supported in part by the National Science Council of R.O.C. under the Grant No. NSC90-2112-M-007-040.

REFERENCES

- [1] For a review, see L.Littenberg and G.Valencia, *Annu. Rev. Nucl. Part. Sci.* **43**, 729 (1993).
- [2] S.L. Glashow, J. Iliopoulos and L. Maiani, *Phys. Rev.* **D 2**, 1585 (1973); M.K. Gaillard and B.W. Lee, *Phys. Rev.* **D 10** 897 (1974), M.K. Gaillard, B.W. Lee and R.E. Shrock, *Phys. Rev.* **D 13**, 2674 (1976); R.E. Shrock and M.B. Voloshin, *Phys. Lett.* **B 87**, 375 (1979).
- [3] C.Q. Geng and J.N. Ng, *Phys. Rev.* **D 41**, 2351 (1990);
- [4] L. Bergstrom, E. Masso, and P. Singer, *Phys. Lett.* **B 249**, 141 (1990); G. Bélanger and C.Q. Geng, *Phys. Rev.* **D 43**, 140 (1991); L. Ritchie and S.G. Wojcicki, *Rev. Mod. Phys.* **65**, 1149 (1993); L. Littenberg and G. Valencia, *Annu. Rev. Nucl. Part. Sci.* **43** 729 (1993).
- [5] G. Valencia, *Nucl. Phys.* **B 517**, 339 (1998).
- [6] P. Ko, *Phys. Rev.* **D 45**, 174 (1992); J.O. Eeg, K. Kumericki and I. Picek, hep-ph/9605337; D. Gomez Dumm and A. Pich, *Phys. Rev. Lett.* **80**, 4633 (1998); M. Knecht, S. Peris, M. Perrottet, and E. de Rafael, *Phys. Rev. Lett.* **83**, 5230 (1999).
- [7] G. D'Ambrosio, G. Isidori, and J. Portoles, *Phys. Lett.* **B 423**, 385 (1998).
- [8] A. Alavi-Harati, *et al.* (KTeV Collaboration), *Phys. Rev. Lett.* **87**, 071801 (2001).
- [9] A. Alavi-Harati, *et al.* (KTeV Collaboration), *Phys. Rev. Lett.* **86**, 5425 (2001).
- [10] A. Lai, *et al.* (NA48 Collaboration), hep-ex/0006040.
- [11] A. Alavi-Harati, *et al.* (KTeV Collaboration), *Phys. Rev. Lett.* **87**, 111802 (2001).
- [12] T. Miyazaki and E. Takasugi, *Phys. Rev.* **D 8**, 2051 (1973).
- [13] L. Zhang and J.L. Goity, *Phys. Lett.* **B 398**, 387 (1997); L. Zhang and J.L. Goity, *Phys. Rev.* **D 57**, 7031 (1998).
- [14] For a review, see B.D. Ksister and W.N. Polyzou, *Adv. Nucl. Phys.* **20**, 225 (1991); F. Coester, *Progress in Part. and Nucl. Phys.* **29**, 1 (1992).
- [15] F. Cardarelli, *et al.*, *Phys. Rev.* **D 53**, 6682 (1996); P.J. O'Donnell, *et al.*, *Phys. Lett.* **B 325**, 219 (1994); N.B. Demchuk, *et al.*, *Phys. Atom. Nucl* **59**, 2152 (1996); C.Y. Cheung, *et al.*, *Z. Phys.* **C 75**, 657 (1997); H.Y. Cheng, *et al.*, *Phys. Rev.* **D 55**, 1559 (1997).
- [16] W. Jaus, *Phys. Rev.* **D 41**, 3394 (1990); *ibid.* **D 44**, 2851 (1991); *Z. Phys.* **C 54**, 611 (1992).
- [17] N.B. Demchuk *et al.*, *Phys. Atom. Nucl* **59**, 2152 (1996).
- [18] C.W. Hwang, hep-ph/0108251.
- [19] C.Y. Cheung, C.W. Hwang, and W.M. Zhang, *Z. Phys.* **C 75**, 657 (1997).
- [20] H.Y. Cheng, C.Y. Cheung, and C.W. Hwang, *Phys. Rev.* **D 55**, 1559 (1997)
- [21] C.W. Hwang, *Phys. Rev.* **D 64**, 034011 (2001).
- [22] H.J. Melosh, *Phys. Rev.* **D 9**, 1095 (1974).
- [23] W. M. Zhang, *Chin. J. Phys.* **31**, 717 (1994); hep-ph/9510428.
- [24] D.E. Groom, *et al.* (Particle Data Group), *Eur. Phys. J.* **C 15**, 1 (2000).
- [25] Cf. H. Lipkin, *Nucl. Phys.* **A675**, 443c (2000), hep-ph/9911246
- [26] E799 Collaboration, N.B. Spencer, *et al.*, *Phys. Rev. Lett.* **74**, 3323 (1995).
- [27] E845 Collaboration, K.E. Ohl, *et al.*, *Phys. Rev. Lett.* **65**, 1407 (1990).
- [28] NA31 Collaboration, C.D. Barr, *et al.*, *Phys. Lett.* **B 240**, 283 (1990).
- [29] Burkhardt H *et al.*, *Phys. Lett.* **B 199**, 139 (1987).
- [30] T. Inami and C. S. Lim, *Prog. Theor. Phys.* **65**, 297 (1981).

- [31] For a recent review, see A.J. Buras, hep-ph/0101336.
- [32] Ll. Ametller, A. Bramon, E. Massó, Phys. Rev. **D 48**, 3388 (1993).
- [33] L. Bergström, *et al.*, Phys. Lett. **B 126**, 117 (1983).
- [34] D. Ambrose *et al.*, E871 Collabration, Phys. Rev. Lett. **81**, 4309 (1998).
- [35] D. Ambrose *et al.*, E871 Collabration, Phys. Rev. Lett. **84**, 1389 (2000).
- [36] G. Buchalla and A.J. Buras, Nucl. Phys. **B412**, 106 (1996); A.J. Buras and R. Fleischer, hep-ph/9704376.
- [37] M. Ciuchini *et al.*, JHEP **0107**, 013 (2001), hep-ph/0012308
- [38] C.Q. Geng and C.W. Hwang, in progress.

FIGURE CAPTIONS

Fig. 1 Feynman diagrams for the meson (a) decay constant and (b) normalization.

Fig. 2 Feynman triangle diagrams with (a) and (b) corresponding to the LF valence configuration. Empty circles indicate LF wave functions.

Fig. 3 The y -dependent behavior of $|f(y)|^2$, where the solid (Model I) and dash (Model II) lines are obtained by this work with $f_K = 159.8\text{MeV}$ and $m_s = 500\text{MeV}$ and the experimental data come from E799 at FNAL [17], E845 at BNL [18], and NA31 at CERN [19], respectively.

FIGURES

FIG. 1.

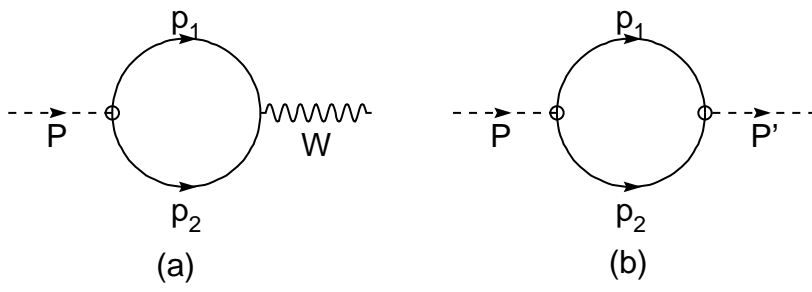


FIG. 2.

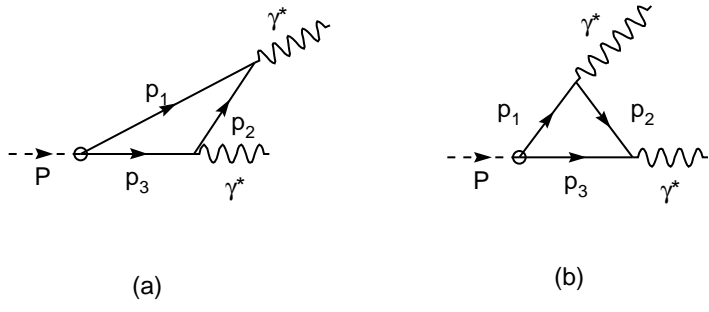


FIG. 3.

